



Published in final edited form as:

J Steroid Biochem Mol Biol. 2019 July ; 191: 105361. doi:10.1016/j.jsbmb.2019.04.010.

Expression of aldosterone synthase CYP11B2 was inversely correlated with longevity

Taiki Hayashi^{a,b}, Zhen Zhang^{a,c}, Ghaith Al-Eyd^d, Atsushi Sasaki^e, Masanori Yasuda^f, Masafumi Oyama^a, Celso E. Gomez-Sanchez^g, Hirotaka Asakura^b, Tsugio Seki^h, Kuniaki Mukai^{i,j,*}, Koshiro Nishimoto^{a,i,**}

^aDepartment of Uro-Oncology, Saitama Medical University International Medical Center, Saitama, Japan

^bDepartment of Urology, Saitama Medical University, Japan

^cTianjin University of Chinese Traditional Medicine, Tianjin, China

^dDepartment of Clinical Science, California Northstate University, Elk Grove, CA, USA

^eDepartment of Pathology, Saitama Medical University, Japan

^fDepartment of Pathology, Saitama Medical University International Medical Center, Japan

^gDivision of Endocrinology, G.V. (Sonny) Montgomery VA Medical Center and University of Mississippi Medical Center, Jackson, MS, USA

^hDepartment of Medical Education, California University of Science and Medicine, San Bernardino, CA, USA

ⁱDepartment of Biochemistry, Keio University School of Medicine, Tokyo, Japan

^jMedical Education Center, Keio University School of Medicine, Tokyo, Japan

Abstract

Immunohistochemistry of human aldosterone synthase (CYP11B2) has revealed that most of aldosterone is autonomously produced in aldosterone-producing cell clusters (APCCs) beneath the capsule of adult adrenals rather than physiologically in the zona glomerulosa (ZG). APCCs have been occasionally found to harbor a somatic mutation of ion channel/pump genes, and number and size of APCCs increase with age until 50 years old. Herein, the objective of the study was to examine APCC development in 106 autopsied adrenals from 85 elderly individuals who died at ages from 50 to 103 years. We obtained the following results: (1) physiological CYP11B2 expression in ZG were attenuated in more elderly persons; (2) number and size of APCCs

*Corresponding author at: Medical Education Center and Department of Biochemistry, Keio University School of Medicine, Tokyo, Japan, k-mukai@keio.jp (K. Mukai). **Corresponding author at: Department of Uro-Oncology, Saitama Medical University International Medical Center, Tokyo, Japan, knishi@saitama-med.ac.jp (K. Nishimoto).

Author contributions

Writing the manuscript: TH, ZZ, TS, HA, CEGS, KM, KN; pathological section preparation: AS; immunohistochemistry: MY; scanning of slides: ZZ; APCC tracing and measuring: KM, KN, GAE; adrenal section tracing and area measuring: ZZ; IRB application: TH, KN, OM; preparation of the HSD3B2 antibody: CEGM.

Disclosure summary

Nothing to disclose.

decreased with age; (3) detachment of APCC from the capsule appeared to occur occasionally over the wide range of the ages; and (4) incidental micro aldosterone-producing adenomas (APAs) and possible APCC-to-APA transitional lesions (pAATLs) were found primarily in samples from persons aged 50–60 years but not in samples from more elderly persons; pAATL was a putative designation based on our previous results indicating that it consisted of subcapsular APCC-like portion and inner APA-like portions. Thus, the formation of the CYP11B2-expressing lesions as well as thickening of the ZG in the adrenals were inversely correlated with age of death in the individuals aged over 50 years. Considering that autopsy samples were used in this study, inactive production of aldosterone regardless of autonomous or physiological manners may have survival advantages in individuals aged over 50 years.

Keywords

Aldosterone-producing cell cluster (APCC); Aldosterone-producing adenoma (APA); Adrenal gland; Aldosterone synthase (CYP11B2)

1. Introduction

1.1. Subtypes of primary aldosteronism

Primary aldosteronism (PA) is the most common cause of secondary hypertension [1,2]. In adults, PA is primarily caused by aldosterone-producing adenoma (APA) or idiopathic hyperaldosteronism (IHA). Somatic mutations in ion channel/pump genes including *KCNJ5* (potassium channel, inwardly rectifying subfamily J, member 5), *ATP1A1* (ATPase Na⁺/K⁺ transporting subunit α 1), *ATP2B3* (ATPase plasma membrane Ca²⁺ transporting 3), *CACNA1D* (calcium voltage-gated channel subunit α 1D), *CACNA1H* (calcium voltage-gated channel subunit α 1H), and *CTNNB1* (catenin β 1) have been identified in adult-onset APAs [3–6]. Juvenile PA is very rare and is mainly caused by four types of familial hyperaldosteronism (types 1–4) [1,2,7]. Among these subtypes of familial PA, familial hyperaldosteronism type 3 is caused by germ-line mutations in ion channel/pump genes including *KCNJ5* [3]. In addition to these PA subtypes, our group has reported an interesting juvenile case of non-familial juvenile PA, which was suggested to be genetic mosaicism of a *KCNJ5* mutation that presumably occurred at mesodermal development [8]. Thus, the causes of PA are currently subclassified into six types (i.e. APA, IHA, and familial hyperaldosteronism types 1–4), whereas the pathology or aldosterone-producing lesions of PA, particularly for IHA, has yet to be elucidated.

1.2. APA, APCC, and pAATL

We previously established immunohistochemistry for aldosterone synthase (CYP11B2) and cortisol-synthesizing enzyme (11 β -hydroxylase, CYP11B1) and achieved a pathological confirmatory diagnosis of APA [9]. APAs contain CYP11B2-expressing cells, CYP11B1-expressing cells, and double negative cells, whereas cortisol-producing adenomas possess CYP11B1-expressing cells and double negative cells [9].

We also reported that sites of CYP11B2 expression in normal adult adrenal glands were mainly aldosterone-producing cell clusters (APCCs) that attached to the capsule rather than

the zona glomerulosa (ZG) [9]. ZG is occasionally discontinuous, and aldosterone synthesis in ZG is mostly uninduced presumably due to autonomous production of aldosterone in APCCs. APCCs morphologically consist of subcapsular ZG-like cells and inner zona fasciculata (ZF)-like cells; the latter cells are histologically indistinguishable from the surrounding ZF cells expressing CYP11B1, thereby making APCCs undetectable with hematoxylin and eosin staining (H&E). They strongly express steroidogenic enzymes necessary for aldosterone synthesis including CYP11B2, but not CYP11B1, suggesting autonomous production of aldosterone [10]. Because they frequently harbor a somatic mutation in one of the ion channel/pump genes, *CACNA1D*, *ATP1A1*, and *ATP2B3*, which were already found in APAs (APA-associated mutations), we suspect that APCCs are precursors of APAs [3–6].

Furthermore, we have proposed possible APCC-to-APA transitional lesion (pAATL) as a putative transitional lesion developing from APCC to APA on the basis of accumulating indirect evidence: Morphological and steroidogenic characteristics of pAATLs indicate that they consist of a subcapsular APCC-like portion and an inner APA-like portion; distributions of somatic mutations of the ion channel/pump genes in the two different portions of pAATLs suggest that APCC is an origin that develops to APA as discussed later [11,12].

The pathologies, namely aldosterone-producing lesions, causing PA (except for familial hyperaldosteronism) have been classified into two categories; one, APAs that unilaterally produce excessive amounts of aldosterone together with different levels of cortisol; and the other, unilateral or bilateral adrenal hyperplasia with micro- and macro-nodules [1,2]. The functional evaluation using immunohistochemistry of CYP11B2 as well as other steroidogenic enzymes allows to revise the conventional classification especially adrenocortical hyperplasia with micro- or macronodules.

1.3. APA-associated mutations

The most frequent APA-associated mutations are those of *KCNJ5* [3]. Mutation of *CACNA1D*, *ATP1A1*, or *ATP2B3* have often been found in the rest of the cohort [4–6]. APCCs of normal individuals were found to have mutations of *the latter three genes* frequently, but not those of *KCNJ5* [10]. Larger pAATLs harbored *KCNJ5* mutations [12]. APAs are generally solitary, whereas multiple APCCs and/or pAATLs often exist together. APAs harboring *KCNJ5*-mutated cells are slightly larger than those of wild-type cells or those with other types of mutations, suggesting that *KCNJ5* renders a proliferative advantage *in vivo* [6,14,15]. On the other hand, Oki et al demonstrated that transduction of HAC15 cells with a lentivirus encoding a *KCNJ5* mutant (p.T158 A) exerted anti-proliferative effects [16]. The mechanisms responsible for the discrepancy of growth effects between *in vitro* and *in vivo* have not yet been elucidated.

1.4. Cell fate in normal adrenal cortex

Previous studies on cell fate of the adrenals of mice indicated that precursor cells located in the subcapsular region differentiated to cells initially expressing CYP11B2, then moved inwards losing the ability to express CYP11B2 but gaining the ability to express CYP11B1 [17,18]. They further migrate centripetally to the cortico-medullary junction, at which they

undergo apoptosis. Human adrenal cortices are assumed to undergo similar phenotypic changes and cell migration, and the cells are possibly removed by apoptosis in the cortico-medullary junction.

Although the fate of APCCs is currently unknown, we previously reported that numbers and sizes of APCCs steadily increase in individuals at least up to 50 years old [19]. Nanba et al. also observed similar changes in APCCs with aging [20]. However, it currently still remains unclear whether APCCs continue to increase in individuals older than 50 years. Therefore, we herein examined expression of CYP11B2 using autopsied adrenals from elderly individuals older than 50 years.

2. Material and methods

2.1. Ethics

The use of human samples in the present study was approved by the Institutional Review Board of the Saitama Medical University International Medical Center (approval #17–197). Animal experiments for immunization and generation of hybridoma cells were performed in the Cell Engineering Corporation (Osaka, Japan) and approved by the Animal Care and Use Committee of the institution as S-251.

2.2. Sample collection

Specimens were from a bank of autopsy samples of the Saitama Medical University Hospital. Cases that had not been diagnosed as PA were retrospectively and randomly selected for this study based on age as follows (Table 1): Two cases each (the newest and second newest) in every age from 50 to 98 years were included, except for 1 case each at ages of 59, 65, 70, 77, 83, 85, 95, and 98 years as well as no case at ages of 82, 93, and 96 years due to the absence of adrenal samples. Additionally, 1 case aged 103 years was included in order to expand the age range. Eighty-five cases comprising 33 females and 52 males were analyzed in the present study. These cases were registered in the database at the Japanese Society of Pathology with specific identification numbers (Byori Boken Syuho, <http://pathology.or.jp/kankoubutu/JSP-hyou.html>) starting with ‘A’ (Table 1 and Supplemental Table 1). Causes of death listed in Table 1 were taken from the database, but not from each patient’s clinical record. One adrenal sample was available from each of 65 cases, while two and three samples were from 19 and 1 cases, respectively (* in Table 1, samples from the left and right adrenals). Serial sections from the 106 adrenal samples were used for histochemical (hematoxylin and eosin) and immunohistochemical analyses (CYP11B2 and HSD3B2), as previously reported [11,21,22]. Images of stained sections were obtained by scanning with the Aperio ScanScope® XT slide scanner (Leica Biosystems, Nussloch, Germany). All scanned images can be downloaded from National Bioscience Database Center in Japan Science and Technology Agency (<https://humandbs.biosciencedbc.jp/en/hum0181-v1>).

2.3. CYP11B2 immunohistochemistry

A mouse monoclonal anti-human CYP11B2 antibody was prepared, validated, and used as described in Supplemental Materials and Methods.

2.4. Sample selection

Sections stained for HSD3B2 were used to exclude non-adrenal samples, low-quality adrenal samples, and less steroid-producing cases. HSD3B2 signal intensities were measured using the Aperio Positive Pixel Count algorithm set in Aperio ImageScope software v.12.2.1.5005 (Leica Biosystems). Briefly, the edge of an HSD3B2-stained adrenal section was traced (green line in Supplemental Fig. 2A), and HSD3B2 signal intensities inside the traced line were converted into pseudo color images (Supplemental Fig. 2A and B images were converted into Supplemental Fig. 2C and D). HSD3B2 positivity was assessed using the Aperio Positive Pixel Count Algorithm, in which areas of weakly positive (yellow in Supplemental Fig. 2D), positive (orange), and strongly positive (red) cells were calculated as follows: positivity = ([area of weakly positive] + [area of positive] + [area of strongly positive]) / ([area of weakly positive] + [area of positive] + [area of strongly positive] + [area of negative]) ('HSD3B2 positivity' in Supplemental Table 1 and Table 1). Thirty-one samples with positivity less than 20% were excluded (*italicized* in Table 1); therefore, 75 samples from 64 cases (24 females and 40 males) were used in analyses (bold in Table 1).

2.5. Measurement of APCC

Three examiners (KN, KM, and GAE) independently recognized and then traced for measurements of sizes and numbers of APCCs on CYP11B2-stained sections using Aperio ImageScope software, as shown in Supplemental Fig. 2E ('APCC area' in Supplemental Table 1). Adrenal areas, percentages of the sum of APCC areas over the whole adrenal area (AA/WAA, %), and numbers of APCCs (NOA/mm²) were calculated and used in statistical analyses as previously reported (Table 1 and Supplemental Table 1). Variations among examiners were primarily due to disagreements in recognition of APCCs; some examiners judged a positive region as APCC and others judged it as a small population of positive cells in ZG. Statistically, NOA (APCCs/mm²) and AA/WAA values from the 3 examiners strongly correlated with each other (r: 0.766 – 0.915, p < 0.0001 in NOA; r: 0.729 – 0.839, p < 0.0001 in AA/WAA; Supplemental Fig. 3), and the average numbers of the three examiners were used for statistical analyses.

2.6. Measurement of CYP11B2-positive ZG thickness

In each sample, three examiners (TS, KM, and GAE) independently selected representative areas of normal ZG, in which no APCC, pAATL, or APA existed, and assessed the representative thickness of CYP11B2-positive ZG for the sample using the following scale: ZG (-) (no positive ZG cells), ZG (+) (0–1 cell layer was positive for CYP11B2), ZG (++) (2–5 cell layers were positive), and ZG (+++) (more than 5 cell layers were positive). Based on the three examiners' measurements, the 'average' ZG thickness for each sample was evaluated by taking the most common assignment, i.e. if two examiners assigned ZG (++) and one examiner assigned ZG (+), the 'average' ZG thickness was ZG (++) . Although the three examiners' measurements agreed in many samples (25 samples, 39%), they assigned three different thicknesses in 6 samples (9%), and, thus, a fourth examiner (KN) independently measured these samples in order to select the most common thickness assignment. Retrospectively, the samples that the three examiners did not agree on mostly had CYP11B2-negative ZG areas with only small areas with positive signals in ZG. Such

samples might lead some examiners to focus their attention incorrectly on the positive areas. All of these samples were assigned ZG (–) when the measurements of the fourth examiner were considered.

2.7. Statistical analysis

Comparisons of AA/WAA and NOA values among the 3 examiners were analyzed by the Kruskal-Wallis one-way analysis of variance on ranks. The relationships between AA/WAA and NOA and between age and AA/WAA or NOA were analyzed by Pearson's product moment correlation. The relationships between NOA or AA/WAA and categorized ZG thickness were analyzed by Spearman's rank order correlation. Comparison of average ages among categorized ZG thickness was analyzed by a one-way analysis of variance. Comparisons of average ages between patients with and without detached APCCs and between patients with and without pAATLs/APA were analyzed using an unpaired Student's *t*-test. P-values less than 0.05 were considered to be significant.

3. Results

3.1. Decrease in numbers and sizes of APCC with age

Adrenal samples from autopsy cases were retrospectively selected for analyses; histological and immunohistochemical staining was performed as previously reported (see images of all samples in Supplemental Fig. 1) [9,10,23]; low-quality samples were excluded (see 'Sample selection' in the Materials and Methods and Supplemental Fig. 2A–D). Percentages of the sum of APCC areas over the whole adrenal area (AA/WAA, %) and numbers of APCCs (NOA, /mm²) were calculated as detailed in the Materials and Methods. Seventy-five samples from 64 cases (24 females and 40 males) with ages ranging from 50 to 103 years were used. Supplemental Fig. 2E shows a representative CYP11B2-stained section used for measurement (APCCs are outlined). Table 1 summarizes patient characteristics and measurement outcomes, and Supplemental Table 1 includes the details of the measurements.

As expected, NOA and AA/WAA strongly correlated ($r = 0.804$, $p = 1.201E-015$, Pearson's product moment correlation analysis), although the r value of males ($r = 0.886$, $p = 3.044E-014$) was greater than that of females ($r = 0.617$, $p = 0.00131$; Fig. 1A). NOA significantly decreased with age ($r = -0.356$, $p = 0.00390$, Pearson's product moment correlation analysis, Fig. 1B). Similarly, AA/WAA significantly decreased with age ($r = -0.316$, $p = 0.0111$, Pearson's product moment correlation analysis, Fig. 1C). When males and females were analyzed separately, the decrease in NOA was significant both in males ($r = -0.391$, $p = 0.0126$) and females ($r = -0.356$, $p = 0.0039$) as well as those in AA/WAA was significant both in males ($r = -0.356$, $p = 0.0243$) and females ($r = -0.316$, $p = 0.0111$). Similar results were observed even including samples which HSD3B2-positivity was larger than 0% (Supplemental Fig. 4A–C) and 10% (Supplemental Fig. 4D–F). These results indicated that the numbers and sizes of APCC decreased with age of death after 50 years old.

3.2. Depression of ZG expression of CYP11B2 with age

In addition to APCCs, the adrenal samples differed in thickness of the CYP11B2-positive ZG layer (Table 1, Supplemental Fig. 1), depending on the physiological upregulation of aldosterone synthesis and responsiveness of ZG, similar to rat adrenals under different conditions of sodium intake [24]. In order to observe age-associated changes, the thickness of representative CYP11B2-positive ZG areas (in which no APCC, pAATL, or APA existed) in each sample was measured as follows: ZG (-) (no positive ZG cells, n = 16, 25%), ZG (+) (0–1 cell layer was positive for CYP11B2, n = 15, 23%), ZG (++) (2–5 cell layers were positive, n = 25, 39%), and ZG (+++) (more than 5 cell layers were positive, n = 8, 13%). Bilateral samples (* in Table 1) generally showed a similar ZG thickness on both sides. Median NOA in ZG (-), ZG (+), ZG (++) and ZG (+++) samples were 0.0101 (0.00303–0.0408) /mm², 0.0248 (0.00944–0.0512) /mm², 0.0332 (0.0199–0.0478) /mm², and 0.0623 (0.0271–0.121) /mm², respectively (Fig. 2A). Accordingly, NOA correlated with ZG thickness (r = 0.389, p = 0.0015; Spearman's rank order correlation). Similarly, median AA/WAA in ZG (-), ZG (+), ZG (++) and ZG (+++) samples were 0.269% (0.0631 – 0.540%), 0.266% (0.127 – 0.783%), 0.371% (0.150 – 0.728%), and 1.09% (0.750–2.45%), respectively (Fig. 2B), and correlated with ZG thickness (r = 0.424, p = 0.000478). These results suggested that the number and size of APCCs were associated with the thickness of CYP11B2-positive ZG. The mean ages of CYP11B2-positive ZG thickness were not significantly different between ZG (-) and ZG (+) (76.7 ± 3.4 [SEM] and 82.3 ± 3.8 years old, respectively, p = 0.228), whereas those of ZG (++) and ZG (+++) were significantly younger than that of ZG (+) (70.2 ± 2.6 and 56.1 ± 1.8 years old, respectively; one-way analysis of variance followed by pairwise multiple comparison procedures with the Holm-Sidak method).

3.3. Detachment of APCC from capsule

APCCs that seemed to be detached from the capsule (pink dotted line in Fig. 3A and B) were detected in 14 cases (21.9%, # in Table 1). The ages of patients with detached APCCs distributed from 51 to 103 years, and the average age of patients with and that without detached APCCs were not significantly different from each other (72.5 [56.5–84.8] and 74.0 [60.0–86.3] years old, respectively, p = 0.826; the Mann-Whitney rank sum test). In addition, an APCC expressing less CYP11B2 (blue-outlined area in Fig. 3C) than other APCCs in the same section (Fig. 3D) was also observed. APCC detachment appeared to occur in a wide age range without age-associated changes. These were the first observations obtained with samples from the elderly.

3.4. Regression of incidental APA with age

We noted that some samples contained non-functional tumors (5 cases, 7.8%) and pAATLs/APAs (6 cases, 9.4%) (Table 1). Multiple pAATLs existed in one case (Fig. 4A, pink arrowheads) and consisted of subcapsular APCC-like portions and inner APA-like portions as previously reported (* and ** in Fig. 4B, respectively) [11,21]. In another case, multiple APCCs (black arrowheads) and pAATLs (pink arrowheads) existed in one adrenal (Fig. 4C). An APA in A-5690 (areas outlined with blue dots in Fig. 4D–F) was found just below a pAATL (the area outlined with red dots in Fig. 4F). This APA might have grown out from

the pAATL because there was no apparent border between these lesions (APCC-like and APA-like lesions are denoted as * and **, respectively, in Fig. 4F). The APA expressed CYP11B2 weakly and heterogeneously, and the positivities of three arbitrarily selected areas were 0, 3, and 17% (boxes in Fig. 4F). The APAs of A-5754 (Fig. 4G and H) and A-5976 (Fig. 4I and J) showed a similar CYP11B2 expression pattern: weak and heterogeneous. An APA of A-5993 showed a stronger expression of CYP11B2, which could have caused PA (Fig. 4K–N). The average age of patients with pAATLs/APAs was significantly younger than those without them (59.8 ± 4.5 and 74.2 ± 4.5 years old, respectively, $p = 0.0227$, unpaired Student's *t*-test), suggesting that APAs are not common in older individuals.

4. Discussion

In the present study, autopsy adrenal samples from patients older than fifty years were employed for examination of CYP11B2 expression with immunohistochemistry. We observed that (1) physiological CYP11B2-positive ZG thickening was less common in the more elderly individuals; (2) numbers and sizes of APCCs decreased with age, particularly in males; (3) detachment and regression of APCC were noted in the adrenals over the wide age range; and (4) incidental pAATLs/APAs were found primarily in samples from patients aged 50–60 years, but not in older individuals. These observations suggest that autonomous aldosterone production as well as physiological production in individuals who live to old ages, such as eighty and older, is less active than those who died earlier.

Direct interpretation of the results may be a notion that the aldosterone-producing lesions or cells regress in life-span of each person with aging after fifty years old. However, since this study used autopsy cases, it is inevitable that the sample collection may be inhomogeneous. Thus, individuals who died later may have fewer or less active aldosterone-producing lesions or cells in the first place than those who died in the fifties. Autonomous aldosterone production may lead to comorbidities and mortalities. In fact, patients with hyperaldosteronism have higher mortality rates [25]. The direct interpretation described above could reflect survival advantages of low levels of aldosterone production.

We previously reported that the NOA and AA/WAA of APCCs steadily increased up to 50 years old using autopsied adrenals [18]. Following our study, Nanba et al. obtained similar findings using normal adrenals from renal transplant donors, who were presumably in good health, thus different from our cohort, aged 9 months to 68 years [20]. Since the two studies carried out with different manners of sample collection gave similar results, it is very likely that numbers and sizes in APCC increased with aging up to fifty years old.

Physiological synthesis of aldosterone in ZG is upregulated by RAS. The current result that the physiological thickening of CYP11B2-positive ZG was diminished in the elderly is consistent with the previous results from human studies showing that RAS is suppressed in elderly individuals [26–29]. Nanba et al. also reported that the adrenals from young renal transplant donors exhibited a layered pattern of CYP11B2 expression in ZG, whereas adrenal glands from older individuals displayed progressively less normal CYP11B2 expression [20]. In addition, they showed that older individuals had less ability to enhance

aldosterone production upon sodium restriction [20], supporting our current results described above.

Immunohistochemistry of CYP11B2 has been changing the conventional concepts of aldosterone production in humans. Subsequently to the discovery of APCC, we further proposed pAATLs as a new form of a culprit lesion [11,12,30]. As described, pAATL was a description by this research group uniquely based on our own data derived from a few cases. Since formation of pAATL seems a transient event, it would be so quite infrequent that researchers seldom encountered with it. One of reasons why we found pAATL would be that we could examine a large number of human adrenals, including so-called adrenal hyperplasia, using in-house generated antibodies to CYP11B2.

In addition to the morphological and steroidogenic characteristics of pAATLs as mentioned earlier, the mutation analyses of the ion channel/pump genes using separately micro-dissected APCC-like portions and APA-like portions gave the following results [31]: (i) Small pAATLs harbor mutations in the genes such as *CACNA1D* except for *KCNJ5*, whereas large pAATLs harbor *KCNJ5* mutations; (ii) mAPA-like portions from two of the three large pAATLs harbored mutations (*KCNJ5* [p.G151R] and *ATP1A1* [p.L337 M]), whereas their corresponding APCC-like portions did not, suggesting their role in the formation of mAPA; (iii) another lesion carried novel mutations in *ATP1A1* (p.Ile322_Ile325del and p.Ile327Ser) in both the mAPA-like and APCC-like portions, thereby supporting these portions having a clonal origin. These findings led us to propose that pAATL could be a candidate for a transitional lesion from APCC to APA. As described, the proposal is supported by the indirect evidence while it has not yet been proven by solid evidence. Thus, it deserves to be a hypothesis for studies on development of culprit lesions causing excessive aldosterone.

Recently, a classical terminology “adrenocortical micronodule” was used for aldosterone-producing lesions [13]. This is a common term of histopathology and lacks functional evaluation for aldosterone production. Since the “micronodules” in the report seemed to consist of APCC-like and micro APA-like portions, they could be called pAATLs according to our definition. Furthermore, in our experiences, so-called adrenal hyperplasia causing PA had morphologically-recognized micronodules negative for CYP11B2 [12] in addition to those positive for it. Thus, the term micronodule may cause confusion in description of pathological PA subtypes. Therefore, the lesions in adrenal hyperplasia can be categorized as APCC, pAATL or small APA based on functional evaluation for expression and distribution of steroidogenic enzymes including CYP11B2. According to the criteria, the pathological classification for PA may be (i) APAs, (ii) multiple APCCs, and (iii) pAATLs.

Lineage tracing studies in mice have shown that the adrenal cells originate in the subcapsular area of the adrenals in which precursor cells differentiate into ZG cells, migrate centripetally with transdifferentiation into ZF cells, and then reach the corticomedullary junction at which they undergo apoptosis [17,18]. These schemes are consistent with the fact that APCCs of humans develop beneath the capsule. On the other hand, a question arises why APCCs do not extend to the bottom of the cortex. Also, the present work raised another question what mechanisms detach APCCs from the capsule, though there was a possibility

that the way to section irregularly-folded adrenals made APCCs look detached. The current detection of the detached APCCs and APCCs with weak-CYP11B2-staining leads us to speculate that they are examples of APCC migrating inward and undergoing de-differentiation or transition to ZF phenotype. Further observational and molecular studies are needed in order to solve the questions, confirm the outcomes of the present study, and prove our hypothesis.

5. Conclusions

The present results suggest that, considering that autopsy samples were used in this study, formation of autonomous lesions for aldosterone production occurred less frequently in individuals who lived to older ages. Inactive production of aldosterone regardless of autonomous or physiological manners may have survival advantages in individuals aged over 50 years.

Supplementary Material

Refer to Web version on PubMed Central for supplementary material.

Acknowledgments

We thank Mr. Kouichi Kamada for his excellent technical help in this study and the China Scholarship Council government for the Scholarship to ZZ (#201,708,785,007). The authors acknowledge funding support from JSPS KAKENHI Grants (to KN [no. 15K10650 and 18K09205] and KM [no. 17K09890]); the Yamaguchi Endocrine Research Foundation (to KN [awarded in 2014 and 2016]); the Okinaka Memorial Foundation (to KN [2016–21]); Ministry of Health, Labor, and Welfare, Japan (Nanbyo-Ippan-046); Federation of National Public Service Personnel Mutual Aid Associations joint research project 2016 (to KN); the National Heart, Lung and Blood Institute R01 HL27255 (to CEGS); and the National Institute of General Medical Sciences U54 GM115428 (to CEGS).

References

- [1]. Funder JW, Carey RM, Fardella C, Gomez-Sanchez CE, Mantero F, Stowasser M, Young WF Jr., Montori VM, Endocrine S, Case detection, diagnosis, and treatment of patients with primary aldosteronism: an endocrine society clinical practice guideline, *J. Clin. Endocrinol. Metab* 93 (2008) 3266–3281. [PubMed: 18552288]
- [2]. Funder JW, Carey RM, Mantero F, Murad MH, Reincke M, Shibata H, Stowasser M, Young WF Jr., The management of primary aldosteronism: case detection, diagnosis, and treatment: an endocrine society clinical practice guideline, *J. Clin. Endocrinol. Metab* 101 (2016) 1889–1916. [PubMed: 26934393]
- [3]. Choi M, Scholl UI, Yue P, Bjorklund P, Zhao B, Nelson-Williams C, Ji W, Cho Y, Patel A, Men CJ, Lolis E, Wisgerhof MV, Geller DS, Mane S, Hellman P, Westin G, Akerstrom G, Wang W, Carling T, Lifton RP, K+ channel mutations in adrenal aldosterone-producing adenomas and hereditary hypertension, *Science* 331 (2011) 768–772. [PubMed: 21311022]
- [4]. Beuschlein F, Boulkroun S, Osswald A, Wieland T, Nielsen HN, Lichtenauer UD, Penton D, Schack VR, Amar L, Fischer E, Walther A, Tauber P, Schwarzmayr T, Diener S, Graf E, Allolio B, Samson-Couterie B, Benecke A, Quinkler M, Fallo F, Plouin PF, Mantero F, Meitinger T, Mulatero P, Jeunemaitre X, Warth R, Vilsen B, Zennaro MC, Strom TM, Reincke M, Somatic mutations in ATP1A1 and ATP2B3 lead to aldosterone-producing adenomas and secondary hypertension, *Nat. Genet* 45 (2013) 440–444 444e441–442. [PubMed: 23416519]
- [5]. Scholl UI, Goh G, Stolting G, de Oliveira RC, Choi M, Overton JD, Fonseca AL, Korah R, Starker LF, Kunstman JW, Prasad ML, Hartung EA, Mauras N, Benson MR, Brady T, Shapiro JR, Loring E, Nelson-Williams C, Libutti SK, Mane S, Hellman P, Westin G, Akerstrom G, Bjorklund P,

- Carling T, Fahlke C, Hidalgo P, Lifton RP, Somatic and germline CACNA1D calcium channel mutations in aldosterone-producing adenomas and primary aldosteronism, *Nat. Genet* 45 (2013) 1050–1054. [PubMed: 23913001]
- [6]. Azizan EA, Poulsen H, Tuluc P, Zhou J, Clausen MV, Lieb A, Maniero C, Garg S, Bochukova EG, Zhao W, Shaikh LH, Brighton CA, Teo AE, Davenport AP, Dekkers T, Tops B, Kusters B, Ceral J, Yeo GS, Neogi SG, McFarlane I, Rosenfeld N, Marass F, Hadfield J, Margas W, Chaggar K, Solar M, Deinum J, Dolphin AC, Farooqi IS, Striessnig J, Nissen P, Brown MJ, Somatic mutations in ATP1A1 and CACNA1D underlie a common subtype of adrenal hypertension, *Nat. Genet* 45 (2013) 1055–1060. [PubMed: 23913004]
- [7]. Daniil G, Fernandes-Rosa FL, Chemin J, Blesneac I, Beltrand J, Polak M, Jeunemaitre X, Boulkroun S, Amar L, Strom TM, Lory P, Zennaro MC, CACNA1H mutations are associated with different forms of primary aldosteronism, *EBioMedicine* 13 (2016) 225–236. [PubMed: 27729216]
- [8]. Tamura A, Nishimoto K, Seki T, Matsuzawa Y, Saito J, Omura M, Gomez-Sanchez CE, Makita K, Matsui S, Moriya N, Inoue A, Nagata M, Sasano H, Nakamura Y, Yamazaki Y, Kabe Y, Mukai K, Kosaka T, Oya M, Suematsu S, Nishikawa T, Somatic KCNJ5 mutation occurring early in adrenal development may cause a novel form of juvenile primary aldosteronism, *Mol. Cell. Endocrinol* 441 (2017) 134–139. [PubMed: 27514282]
- [9]. Nishimoto K, Nakagawa K, Li D, Kosaka T, Oya M, Mikami S, Shibata H, Itoh H, Mitani F, Yamazaki T, Ogishima T, Suematsu M, Mukai K, Adrenocortical zonation in humans under normal and pathological conditions, *J. Clin. Endocrinol. Metab* 95 (2010) 2296–2305. [PubMed: 20200334]
- [10]. Nishimoto K, Tomlins SA, Kuick R, Cani AK, Giordano TJ, Hovelson DH, Liu CJ, Sanjanwala AR, Edwards MA, Gomez-Sanchez CE, Nanba K, Rainey WE, Aldosterone-stimulating somatic gene mutations are common in normal adrenal glands, *Proceedings of the National Academy of Sciences of the United States of America* 112 (2015) E4591–E4599. [PubMed: 26240369]
- [11]. Nishimoto K, Koga M, Seki T, Oki K, Gomez-Sanchez EP, Gomez-Sanchez CE, Naruse M, Sakaguchi T, Morita S, Kosaka T, Oya M, Ogishima T, Yasuda M, Suematsu M, Kabe Y, Omura M, Nishikawa T, Mukai K, Immunohistochemistry of aldosterone synthase leads the way to the pathogenesis of primary aldosteronism, *Mol. Cell. Endocrinol* 441 (2017) 124–133. [PubMed: 27751767]
- [12]. Nishimoto K, Seki T, Kurihara I, Yokota K, Omura M, Nishikawa T, Shibata H, Kosaka T, Oya M, Suematsu M, Mukai K, Case report: nodule development from subcapsular aldosterone-producing cell clusters causes hyperaldosteronism, *J. Clin. Endocrinol. Metab* 101 (2016) 6–9. [PubMed: 26580238]
- [13]. Yamazaki Y, Nakamura Y, Omata K, Ise K, Tezuka Y, Ono Y, Morimoto R, Nozawa Y, Gomez-Sanchez CE, Tomlins SA, Rainey WE, Ito S, Satoh F, Sasano H, Histopathological classification of cross-sectional image-negative hyperaldosteronism, *J. Clin. Endocrinol. Metab* 102 (2017) 1182–1192. [PubMed: 28388725]
- [14]. Fernandes-Rosa FL, Williams TA, Riestler A, Steichen O, Beuschlein F, Boulkroun S, Strom TM, Monticone S, Amar L, Meatchi T, Mantero F, Cicala MV, Quinkler M, Fallo F, Allolio B, Bernini G, Maccario M, Giacchetti G, Jeunemaitre X, Mulatero P, Reincke M, Zennaro MC, Genetic spectrum and clinical correlates of somatic mutations in aldosterone-producing adenoma, *Hypertension* 64 (2014) 354–361. [PubMed: 24866132]
- [15]. Zennaro MC, Boulkroun S, Fernandes-Rosa F, Genetic causes of functional adrenocortical adenomas, *Endocr. Rev* 38 (2017) 516–537. [PubMed: 28973103]
- [16]. Oki K, Plonczynski MW, Luis Lam M, Gomez-Sanchez EP, Gomez-Sanchez CE, Potassium channel mutant KCNJ5 T158A expression in HAC-15 cells increases aldosterone synthesis, *Endocrinology* 153 (2012) 1774–1782. [PubMed: 22315453]
- [17]. Freedman BD, Kempna PB, Carlone DL, Shah MS, Guagliardo NA, Barrett PQ, Gomez-Sanchez CE, Majzoub JA, Breault DT, Adrenocortical zonation results from lineage conversion of differentiated zona glomerulosa cells, *Dev. Cell* 26 (2013) 666–673. [PubMed: 24035414]
- [18]. King P, Paul A, Laufer E, Shh signaling regulates adrenocortical development and identifies progenitors of steroidogenic lineages, *Proceedings of the National Academy of Sciences of the United States of America* 106 (2009) 21185–21190. [PubMed: 19955443]

- [19]. Nishimoto K, Seki T, Hayashi Y, Mikami S, Al-Eyd G, Nakagawa K, Morita S, Kosaka T, Oya M, Mitani F, Suematsu M, Kabe Y, Mukai K, Human adrenocortical remodeling leading to aldosterone-producing cell cluster generation, *Int. J. Endocrinol* 2016 (2016) 7834356. [PubMed: 27721827]
- [20]. Nanba K, Vaidya A, Williams GH, Zheng I, Else T, Rainey WE, Age-related autonomous aldosteronism, *Circulation* 136 (2017) 347–355. [PubMed: 28566337]
- [21]. Makita K, Nishimoto K, Kiriyama-Kitamoto K, Karashima S, Seki T, Yasuda M, Matsui S, Omura M, Nishikawa T, A novel method: super-selective adrenal venous sampling, *J. Vis. Exp* 15 (9 (127)) (2017), 10.3791/55716.
- [22]. Gomez-Sanchez CE, Lewis M, Nanba K, Rainey WE, Kuppusamy M, Gomez-Sanchez EP, Development of monoclonal antibodies against the human 3beta-hydroxysteroid dehydrogenase/isomerase isozymes, *Steroids* 127 (2017) 56–61. [PubMed: 28863887]
- [23]. Uchida N, Amano N, Yamaoka Y, Uematsu A, Sekine Y, Suzuki M, Watanabe J, Nishimoto K, Mukai K, Fukuzawa R, Hasegawa T, Ishii T, A novel case of somatic KCNJ5 mutation in Pediatric-Onset Aldosterone-Producing Adenoma, *J. Endocr. Soc* 1 (2017) 1056–1061. [PubMed: 29264557]
- [24]. Nishimoto K, Harris RB, Rainey WE, Seki T, Sodium deficiency regulates rat adrenal zona glomerulosa gene expression, *Endocrinology* 155 (2014) 1363–1372. [PubMed: 24422541]
- [25]. Reincke M, Fischer E, Gerum S, Merkle K, Schulz S, Pallauf A, Quinkler M, Hanslik G, Lang K, Hahner S, Allolio B, Meisinger C, Holle R, Beuschlein F, Bidlingmaier M, Endres S, Observational study mortality in treated primary aldosteronism: the German Conn's registry, *Hypertension* 60 (2012) 618–624. [PubMed: 22824982]
- [26]. Weidmann P, De Myttenaere-Bursztejn S, Maxwell MH, de Lima J, Effect on aging on plasma renin and aldosterone in normal man, *Kidney Int.* 8 (1975) 325–333. [PubMed: 538]
- [27]. Hegstad R, Brown RD, Jiang NS, Kao P, Weinshilboum RM, Strong C, Wisgerhof M, Aging and aldosterone, *Am. J. Med* 74 (1983) 442–448. [PubMed: 6338717]
- [28]. Tsunoda K, Abe K, Goto T, Yasujima M, Sato M, Omata K, Seino M, Yoshinaga K, Effect of age on the renin-angiotensin-aldosterone system in normal subjects: simultaneous measurement of active and inactive renin, renin substrate, and aldosterone in plasma, *J. Clin. Endocrinol. Metab* 62 (1986) 384–389. [PubMed: 3510226]
- [29]. Crane MG, Harris JJ, Effect of aging on renin activity and aldosterone excretion, *J. Lab. Clin. Med* 87 (1976) 947–959. [PubMed: 932525]
- [30]. Zhang Z, Sugiura Y, Mune T, Nishiyama M, Terada Y, Mukai K, Nishimoto K, Immunohistochemistry for aldosterone synthase CYP11B2 and matrix-assisted laser desorption ionization imaging mass spectrometry for in-situ aldosterone detection, *Curr. Opin. Nephrol. Hypertens.* 28 (3 (2)) (2019) 105–112.
- [31]. Nishimoto K, Seki T, Kurihara I, et al., Case report: nodule development from subcapsular aldosterone-producing cell clusters causes hyperaldosteronism, *J. Clin. Endocrinol. Metab* 101 (1) (2016) 6–9. [PubMed: 26580238]

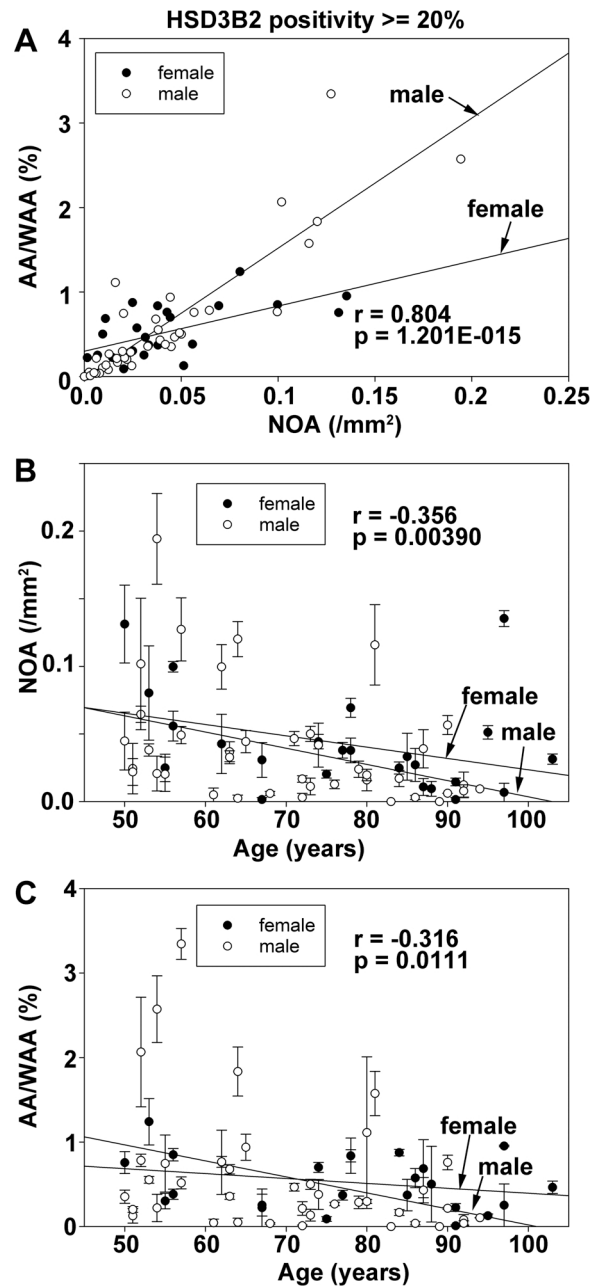


Fig. 1.

Relationship between adrenal senescence and APCCs.

A: Correlation between the average value of AA/WAA (%) and that of NOA (/mm²). B:

Correlation between age (years) and NOA (/mm²) with the SEM of three examiners. C:

Correlation between age (years) and AA/WAA (%) with the SEM of three examiners.

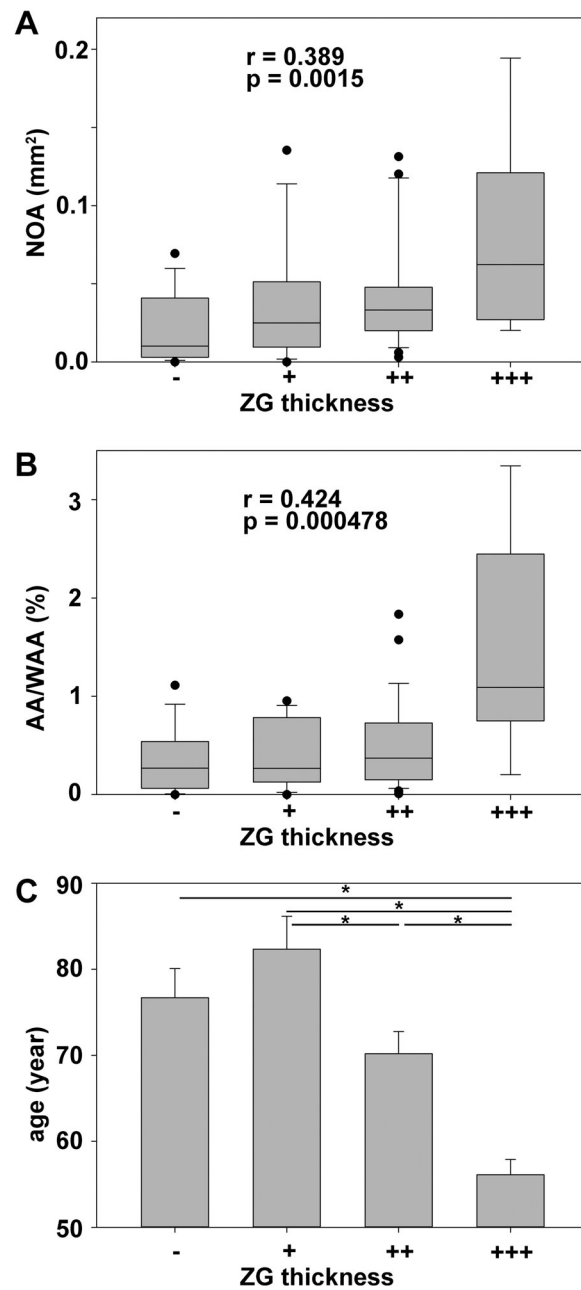


Fig. 2.
ZG thickness vs NOA, AA/WAA, and age.

A and B: Correlation between NOA and ZG thickness and between AA/WAA and ZG thickness, respectively. The boundary of the box indicates the 25th and 75th percentiles, and the line within the box marks the median. Whiskers below and above the box indicate the 10th and 90th percentiles, respectively. r and p values were calculated by Spearman's rank order correlation analysis. C: Correlation between age and ZG thickness. Bars and error bars indicate the average and SEM, respectively. These average values were compared by a one-way analysis of variance followed by pairwise multiple comparison procedures (Holm-Sidak method). “*” indicates a significant difference between the ZG thickness groups.

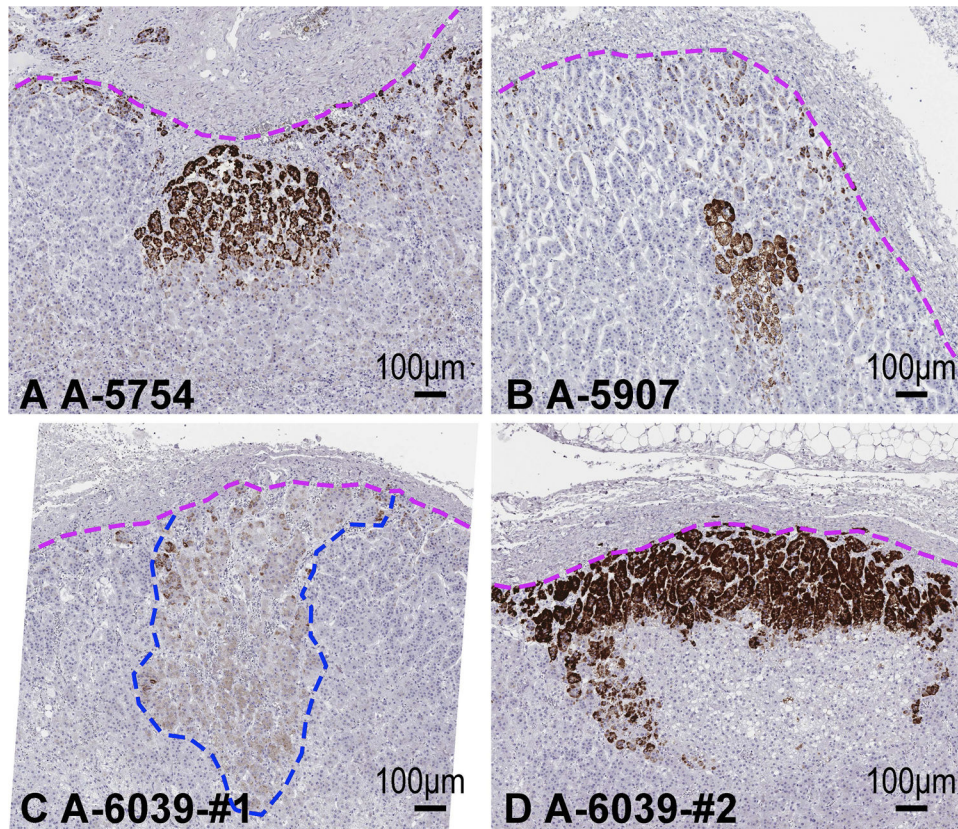


Fig. 3.

Detached and disappearing APCCs.

A and B: APCCs detached from the adrenal capsule (pink dotted line) in samples A-5754 (A) and A-5907 (B). C and D: APCC with weaker CYP11B2 expression (C) than another APCC (D) in the same A-6039 section. A large APCC in D is shown with cells that are migrating into the zona fasciculata.

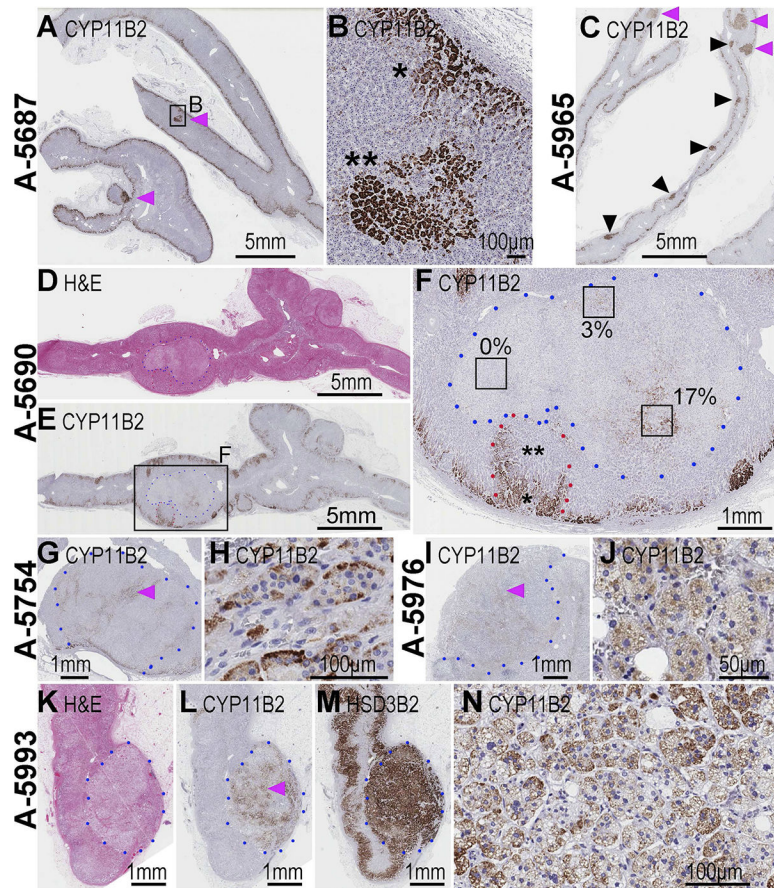


Fig. 4.

pAATLs and incidental APAs.

A: An example of a pAATL (purple arrowheads). A frame indicating the portion of the enlarged image in panel B. B: An enlarged pAATL, which consisted of a subcapsular APCC-like portion and inner APA-like portion. C: Another example of a pAATL (pink arrowheads). This sample had multiple APCCs. D and E: Hematoxylin and eosin staining (H&E) and CYP11B2 staining of an adrenal with pAATL (surrounded by red dots) and incidental APA (surrounded by blue dots), respectively. A frame indicating the enlarged image in panel F. F: Enlarged image of pAATL (surrounded by red dots) and incidental APA (surrounded by blue dots), which were histologically separated from each other. Frames with percentages indicate the positivity of CYP11B2. G and H: An incidental APA with a small CYP11B2-positive area and its enlarged image (pink arrowhead in G), respectively. I and J: Another incidental APA with a small CYP11B2-positive area and its enlarged image (pink arrowhead in I), respectively. K-M: H&E, CYP11B2 staining, and HSD3B2 staining of an incidental APA with a relatively large area positive for CYP11B2. The pink arrowhead in panel L indicates the enlarged image in panel N.

Table 1:

Case characteristics.

Case_ID	sex	age	cause of death	block number	other lesions	ZG thickrless statistics	KN	KM	TS	GAE	HSD3B2 positivity	NOA (APCCs/mm ² , mean ± S.E.M.)	AA/WAA (% mean ± S.E.M.)	Figure
A-3944	* female	95	uterine cervical cancer	12		+					0.351	0.0512 ± 0.0049	0.1269 ± 0.0213	
A-4165	male	89	cholangiocarcinoma	13		+					0.288	0 ± 0	0 ± 0	
A-4617	* male	89	brain infarction	32							0.065	0.0088 ± 0.0047	0.077 ± 0.0487	
A-4769	* female	94	chronic heart failure	33							0.158			
A-5092	* female	97	congestive heart failure, aortic stenosis,	22		-					0.214	0.0068 ± 0.0068	0.2515 ± 0.2515	
A-5400	# male	92	colon cancer, liver metastasis	23	non func T	++					0.14	0.0123 ± 0.0094	0.0807 ± 0.0602	
A-5407	male	98	brain infarction								0.484	0.0043 ± 0.0043	0.0026 ± 0.0026	
A-5454	female	91	acute myocardial infarction			+					0.126	0.0145 ± 0.0029	0.2248 ± 0.0455	
A-5550	female	50	T-cell lymphoma			++					0.202	0.1313 ± 0.0288	0.7565 ± 0.1301	
A-5576	* male	52	sudden death	29		+					0.384	0.0645 ± 0.006	0.7828 ± 0.0736	
A-5624	male	51	lung cancer	51		-	+	-	++		0.43			
A-5687	# male	55	sepsis due to pneumonia		pAATL	++					0.288	0.0244 ± 0.0186	0.1267 ± 0.0861	
A-5690	* male	52	septic shock	4	APA	+++					0.406	0.0202 ± 0.0127	0.7461 ± 0.3369	4A-B
A-5699	male	94	senility	5							0.437	0.1018 ± 0.0487	2.0654 ± 0.6485	4D-F
A-5737	* female	91	pancreatic cancer	18		-					0.359	0.0093 ± 0	0.104 ± 0.0031	
				19		-					0.287	0.0015 ± 0.0015	0.0091 ± 0.0091	
											0.452			
											0.431			

Case_ID	sex	age	cause of death	block number	other lesions	ZG thickrless statistics	KN	KM	TS	GAE	HSD3B2 positivity	NOA (APCCs/mm ² , mean ± S.E.M.)	AA/WAA (% , mean ± S.E.M.)	Figure
A-5746	male	86	infectious endocarditis		non func T	+					0.407	0.003 ± 0.0015	0.0375 ± 0.0192	
A-5754	male	51	liver cirrhosis		APA	+++					0.464	0.0219 ± 0.0099	0.2022 ± 0.0333	3 A, 4 G-H
A-5790	female	103	brain tumor			+					0.245	0.0314 ± 0.0038	0.4637 ± 0.0735	
A-5797	male	53	pyothorax	12		-					0.312	0.0381 ± 0.0046	0.5531 ± 0.0403	
				13							0.279			
A-5814	male	90	primary macroglobulinemia			-					0.264	0.0061 ± 0	0.2154 ± 0.0106	
A-5843	male	92	pneumonia, choronic heart failure			+					0.369	0.0078 ± 0.0045	0.0388 ± 0.0275	
A-5845	male	60	sepsis	16							0.056	0.0047 ± 0.0009	0.06 ± 0.0147	
				17							0.104			
A-5846	male	60	systemic lupus erythematosus								0.044	0.0021 ± 0.0021	0.0108 ± 0.0108	
A-5847	male	50	dermatomyositis, interstitial pneumonia		non func T	++					0.22	0.0448 ± 0.0213	0.3531 ± 0.0786	
A-5850	male	63	T-cell lymphoma			++					0.223	0.0368 ± 0.0074	0.678 ± 0.0553	
A-5853	male	62	rupture of esophagus varix, liver cirrhosis			++					0.463	0.0995 ± 0.0165	0.7657 ± 0.0651	
A-5861	male	58	Fournier's gangrene								0.157	0 ± 0	0 ± 0	
A-5864	male	87	tuberculous pleuritis			+					0.282	0.039 ± 0.0142	0.4301 ± 0.1498	
A-5869	male	63	multiple myeloma			++					0.285	0.0327 ± 0.0047	0.3572 ± 0.0341	
A-5876	female	86	sepsis			++					0.355	0.0271 ± 0.0122	0.5739 ± 0.1134	
A-5885	male	66	toxic epidermal necrolysis								0.107	0.0058 ± 0.0058	0.024 ± 0.024	
A-5886	male	54	mediastinal tumor	38		+++					0.357	0.1943 ± 0.0335	2.5731 ± 0.3939	
				39							0.309			
A-5890	male	90	chronic obstructive pulmonary disease			++					0.336	0.0566 ± 0.007	0.7581 ± 0.0861	

Case_ID	sex	age	cause of death	block number	other lesions	ZG thickrless statistics	KN	KM	TS	GAE	HSD3B2 positivity	NOA (APCC-s/mm ² , mean ± S.E.M.)	AA/WAA (% , mean ± S.E.M.)	Figure
A-5900	*	71	origin unknown cancer	4							0.092	0 ± 0	0 ± 0	
				5							0.082			
				6							0.014			
A-5907	#	87	origin unknown cancer			-					0.381	0.0108 ± 0.0062	0.6849 ± 0.3427	3B
A-5918		75	angina pectoris								0.038	0 ± 0	0 ± 0	
A-5933	*	84	hepatocellular cancer	24		++					0.219	0.0171 ± 0.0059	0.1658 ± 0.0348	
				25							0.379			
A-5940	*	68	acute myeloid leukemia	48		++					0.305	0.006 ± 0.0015	0.0366 ± 0.008	
				49							0.2			
A-5942		54	diabetes mellitus, chronic renal failure			++					0.205	0.0207 ± 0.0129	0.2199 ± 0.1623	
A-5947		70	T-cell lymphoma			+++					0.032	0.0338 ± 0.0135	0.4776 ± 0.0516	
A-5950		53	aplastic anemia								0.458	0.0803 ± 0.0349	1.2402 ± 0.2748	
A-5956	*	58	Wegener's granulomatosis	37							0.183	0.0337 ± 0.0148	0.3076 ± 0.1402	
				38							0.143			
A-5965		57	autoimmune hemolytic anemia		PAAATL/ APA	+++					0.209	0.1273 ± 0.0233	3.3451 ± 0.1821	4C
A-5972		55	sepsis			++					0.247	0.0249 ± 0.0101	0.302 ± 0.0909	
A-5976		64	multiple myeloma		APA	-					0.326	0.0024 ± 0.0024	0.0494 ± 0.0494	4I-J
A-5980		64	sepsis			++					0.272	0.1202 ± 0.013	1.8349 ± 0.2901	
A-5987		56	heart failure, hyperkalemia			-	-	++	-	+	0.315	0.0558 ± 0.0111	0.3821 ± 0.0601	
A-5989		74	heart failure, pneumonia			++					0.275	0.0443 ± 0.0053	0.7004 ± 0.0582	
A-5992		56	fulminant hepatitis			+					0.426	0.0997 ± 0.0038	0.8492 ± 0.0739	
A-5993		80	multiple organ failure		APA	-					0.438	0.016 ± 0.008	1.1119 ± 0.8975	4K-N
A-5994		81	aspiration pneumonia			++					0.254	0.1159 ± 0.0297	1.5742 ± 0.2628	

Case_ID	sex	age	cause of death	block number	other lesions	ZG thickrless statistics	KN	KM	TS	GAE	HSD3B2 positivity	NOA (APCC-s/mm ² , mean ± S.E.M.)	AA/WAA (% mean ± S.E.M.)	Figure
A-5996	*	69	follicular lymphoma	23							0.199	0.0299 ± 0.0069	0.4409 ± 0.0677	
				24							0.186			
A-6004	male	76	post surgical hemorrhage, gastric			+					0.394	0.0127 ± 0.0032	0.2663 ± 0.0198	
A-6007	* # female	77	colon cancer, liver metastasis	22	non func T	++					0.47	0.0379 ± 0.0058	0.371 ± 0.058	
A-6012	* female	68	rectal ulcer, hepatic abscess	21	non func T						0.158	0 ± 0	0 ± 0	
A-6017	female	88	toxic epidermal necrolysis	22							0.108	0 ± 0	0 ± 0	
A-6020	* male	71	infectious aortic aneurism	21		++					0.309	0.0465 ± 0.0052	0.4653 ± 0.0461	
A-6025	female	79	pancreatic cancer, liver metastases	22							0.003	0 ± 0	0 ± 0	
A-6026	female	69	remitting seronegative symmetrical synovitis with pitting edema								0.119	0.0781 ± 0.0232	0.8481 ± 0.2656	
A-6028	male	66	hemorrhagic shock								0.178	0.0259 ± 0	0.7815 ± 0.0942	
A-6030	male	63	interstitial pneumonia								0.173	0.0615 ± 0.009	0.5256 ± 0.0573	
A-6031	female	88	hepatocellular cancer			+					0.274	0.0094 ± 0.0054	0.5015 ± 0.4482	
A-6032	female	97	gastric submucosal tumor		non func T	+					0.648	0.1354 ± 0.0059	0.9525 ± 0.0093	
A-6033	female	78	autoimmune hemolytic anemia			++					0.245	0.0378 ± 0.0091	0.8364 ± 0.0723	
A-6037	# male	73	carbon dioxide narcosis			-	+	-	++		0.379	0.05 ± 0.0056	0.4996 ± 0.0599	
A-6039	# female	78	multiple myeloma			-	+	-	++		0.386	0.0693 ± 0.007	0.8375 ± 0.2084	3C-D

Case_ID	sex	age	cause of death	block number	other lesions	ZG thickrless statistics	KN	KM	TS	GAE	HSD3B2 positivity	NOA (APCC-s/mm ² , mean ± S.E.M.)	AA/WAA (% , mean ± S.E.M.)	Figure
A-6041	male	79	lung tumor		non adrenal T	-					0.22	0.0239 ± 0.006	0.2863 ± 0.0744	
A-6043	# male	83	acute leukemia			-	-	+	-	+++	0.42	0 ± 0	0	0
A-6044	# male	72	pneumonia			+					0.349	0.0167 ± 0.0024	0.2135 ± 0.0794	
A-6045	# male	57	pneumonia			++					0.324	0.0491 ± 0.0064	0.5166 ± 0.0702	
A-6049	female	81	multiple system atrophy								0.093	0.0327 ± 0.003	0.795 ± 0.2027	
A-6050	female	76	acute myocardial infarction, multiple organ failure								0.043	0 ± 0	0 ± 0	0
A-6054	female	67	idiopathic bacterial peritonitis			+					0.551	0.0307 ± 0.0129	0.2537 ± 0.1297	
A-6055	male	74	rheumatoid arthritis, interstitial pneumonia			-	-	+++	-	++	0.364	0.0417 ± 0.0163	0.3794 ± 0.1781	
A-6056	female	75	myelodysplastic syndromes, sepsis			++					0.356	0.0203 ± 0.0029	0.0892 ± 0.0282	
A-6058	# male	72	multiple hepatic metastases of origin unknown carcinoma			++					0.287	0.003 ± 0.003	0.0083 ± 0.0083	
A-6060	female	67	ovarian tumor			-					0.236	0.0015 ± 0.0015	0.2219 ± 0.2219	
A-6061	* female	62	small-intestinal hemorrhage	17		+++					0.442	0.0426 ± 0.0219	0.7604 ± 0.3806	
A-6062	male	73	pulmonary fibrosis	18		++					0.563	0.0111 ± 0.0062	0.1348 ± 0.0706	
A-6063	# female	84	systemic lupus erythematosus			+					0.305	0.0248 ± 0.0045	0.8752 ± 0.039	
A-6066	male	61	multiple myeloma			-					0.344	0.005 ± 0.005	0.044 ± 0.044	
A-6068	male	5	hepatocellular cancer			+++					0.37	0.0443 ± 0.0082	0.9379 ± 0.1536	
A-6069	female	85	diffuse large B-cell lymphoma			++					0.451	0.0332 ± 0.0173	0.3724 ± 0.1863	
A-6071	male	80	aspiration pneumonitis			++					0.312	0.0196 ± 0.0043	0.297 ± 0.0248	

Case_ID	sex	age	cause of death	block number	other lesions	ZG thickrless statistics	KN	KM	TS	GAE	HSD3B2 positivity	NOA (APCCs/mm ² , mean ± S.E.M.)	AA/WAA (% , mean ± S.E.M.)	Figure	
A-6072	*	59	<i>diffuse large B-cell lymphoma</i>	35							0.026	0	± 0	0	± 0
				36							0.177				

NOA: number of APCCs/mm², AA/WAA: APCC area per whole adrenal area (%),

*: cases who had 2–3 sample blocks,

#: samples with detached APCCs, n.a.: not available, bold characters: HSD3B2-positivity>=20%, italic characters: HSD3B2-positivity<20%.